

Single-photon light detection with transition-edge sensors

M. RAJTERI, E. TARALLI, C. PORTESI and E. MONTICONE

Istituto Nazionale di Ricerca Metrologica INRIM - Strada delle Cacce 91, 10135 Torino, Italy

(ricevuto il 12 Gennaio 2009; approvato il 28 Gennaio 2009; pubblicato online il 4 Marzo 2009)

Summary. — Transition-Edge Sensors (TESs) are microcalorimeters that measure the energy of incident single photons by the resistance increase of a superconducting film biased within the superconducting-to-normal transition. TES are able to detect single photons from IR to X-ray with an intrinsic energy resolution and photon-number discrimination capability. Metrology, astronomy and quantum communication are the fields where these properties can be particularly useful. In this work, we report about characterization of different TESs based on Ti films. Single photons have been detected from 200 nm to 800 nm working at transition temperature $T_c \sim 100$ mK. Using a pulsed laser at 690 nm we have demonstrated the capability to resolve up to five photons.

PACS 07.20.Mc – Cryogenics; refrigerators, low-temperature detectors, and other low-temperature equipment.

PACS 85.25.0j – Superconducting optical, X-ray, and γ -ray detectors (SIS, NIS, transition edge).

1. – Introduction

Nowadays in many scientific fields, like astronomy, metrology, quantum computation and quantum information, to extend the knowledge it is necessary to work at the level of single photons. This means that a lot of efforts have to be done to develop both single-photon sources and detectors [1]. On the detector side the requirements are for high quantum efficiency and intrinsic energy resolution or photon-number resolving capability from the UV down to the IR region. At the moment, even if improvements on both semiconducting and superconducting devices are in progress [1], these performances can be obtained only with superconducting devices and in particular with Transition-Edge Sensors (TESs). TESs are microcalorimeters that measure the energy of incident single photons by the resistance increase of a superconducting film biased within the superconducting-to-normal transition. With a proper heat capacity C , TESs are able to detect single photons from IR to X-ray with an intrinsic energy resolution and photon-number discrimination capability.

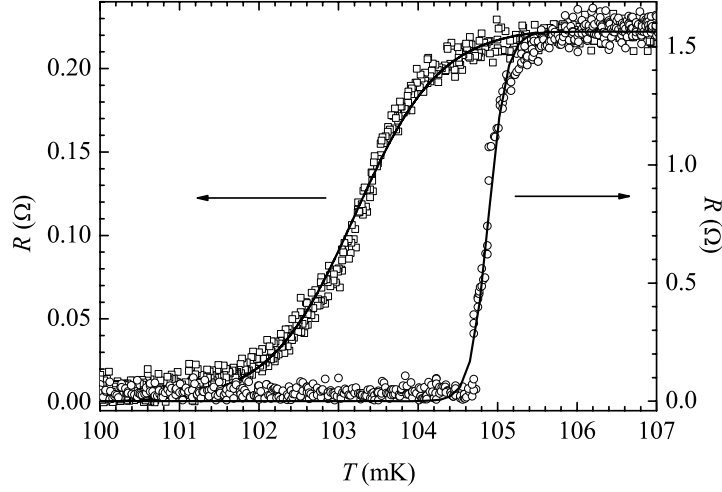


Fig. 1. – TES resistance *vs.* sensor temperature for TiAu (open square) and TiPd (open circle) bilayers. Solid lines show the fit function described in the text with $a = 1.56 \Omega$, $k = 8.96 \text{ mK}^{-1}$, $T_c = 104.8 \text{ mK}$ for the TiPd sample and $a = 0.224 \Omega$, $k = 1.86 \text{ mK}^{-1}$, and $T_c = 103.2 \text{ mK}$ for the TiAu TES.

In this work, we report about the characterization of TESs developed at INRIM using two different non-magnetic metals, Au and Pd, to reduce the transition temperature of the superconducting material Ti. TESs with T_c ranging between 300 mK to tens of mK have been obtained. In the following single-photon measurements are presented, obtained with TESs having a $T_c \sim 100 \text{ mK}$.

2. – Description

We have fabricated and characterized different $20 \mu\text{m} \times 20 \mu\text{m}$ TESs consisting of Ti/Au/Ti and Ti/Pd/Ti multilayers sequentially evaporated by e-gun on $500 \mu\text{m}$ double-side polished Si wafer covered on both sides by 500 nm thick SiN layer grown by LPCVD. More details about the fabrication of the devices are reported in other works [2, 3]. We report here results obtained with Ti(15 nm)/Au(72 nm)/Ti(55 nm) TES and Ti(15 nm)/Pd(16 nm)/Ti(65 nm) TES with a transition temperature T_c of 103.2 mK and 104.8 mK, respectively. Their resistance R *vs.* temperature T curves are reported in fig. 1. The experimental data can be fitted with the function $R(T) = a/\{1 + \exp[-k(T - T_c)]\}$, where a and k are constants; from the fit we can evaluate $\Delta T_c = 0.5 \text{ mK}$ and 2 mK and a normal resistance $R_N = 1.56 \Omega$ and 0.224Ω for TiPd and TiAu TES, respectively. The sensor resistance was measured using four wire readout and lock-in amplifier with typical sinusoidal excitation current of $0.2 \mu\text{A}$ at 37 Hz.

In fig. 2 is shown the electrical circuit used to bias the device and to read out the signal. $R_{\text{bias}} = 9.5 \text{ m}\Omega$ is much lower than the TESs normal resistance and allows to transform the bias current I_{bias} into a bias voltage V_{bias} for the sensor. When the TES resistance rises due to an absorbed photon, we have a sudden decrease of I_{tes} and consequently the electrical power $P = V_{\text{bias}}^2/R_{\text{tes}}$ diminishes because the V_{bias} is fixed and the TES resistance is increased. The energy deposited into the film is approximately the integral of the current pulse. The variation of I_{tes} is read out using a DC SQUID amplifier running

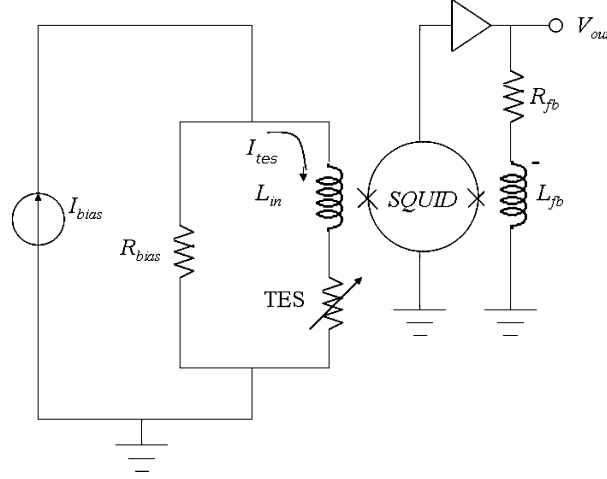


Fig. 2. – ETF-TES bias circuit with SQUID read out.

in flux-locked loop mode through feedback resistor R_{fb} . This type of polarization is called negative Electro-Thermal Feedback (ETF) [4] and allows to obtain a self-regulation of the bias point without a fine temperature control if the bath temperature is lower than the sensor transition temperature.

The current pulse, obtained from the photon absorption, is characterized by a rise time constant dependent on the bias circuit parameters $\tau_{el} = L/[R_{bias} + R_0(1 + \beta)]$, where L is the sum of the SQUID input coil and any stray inductance of the entire bias circuit, R_{bias} is the resistance of the bias circuit, R_0 is the detector resistance at the working point, and β is the current sensitivity at constant temperature [5]. In the case of strong ETF the effective response time can be expressed as $\tau_{etf} = \tau_{th}/(\ell + 1)$, where $\ell = \alpha R_{tes} I_{tes}^2 / GT_c$ is the loop gain, $\alpha = (T_0/R_0)(dR/dT)$ the logarithmic sensitivity of the thermometer, and τ_{th} is the thermal time constant.

To choose the working point of our device as single-photon detector, we studied the trend of the current I_{tes} through the TES as a function of the bias current I_{bias} , as shown in fig. 3 for TiAu TES. In the figure, we can distinguish at low I_{bias} values the superconducting vertical region, except for a parasitic resistance of $\sim 6 \text{ m}\Omega$; for $I_{bias} > 100 \mu\text{A}$ a normal region, corresponding to the 0.225Ω straight line, is observed. The intermediate region corresponds to the superconducting to normal transition. Measurements of such characteristics at different temperatures provide information about resistance, thermal coupling, dissipated power and electrothermal feedback in TES; for our Ti/Au and Ti/Pd TES we can estimate a detector thermal conductance $G = 15.3 \text{ pW/K}$ and $G = 8.42 \text{ pW/K}$ [6].

The heat capacity C of our TESs is calculated as the sum of every layer capacity where a factor 2.43 takes into account the increase of the heat capacity of the superconducting material at the transition temperature [7]. For the case of Ti/Au TES we have $C = 2.45 \text{ fJ/K}$ and for the case of Ti/Pd TES, we have $C = 3.3 \text{ fJ/K}$. Now it is possible to estimate the thermal time constant $\tau_{th} = C/G$ of our detectors by the ratio of their thermal properties obtaining $160 \mu\text{s}$ and $391 \mu\text{s}$ for Ti/Au and Ti/Pd TES, respectively.

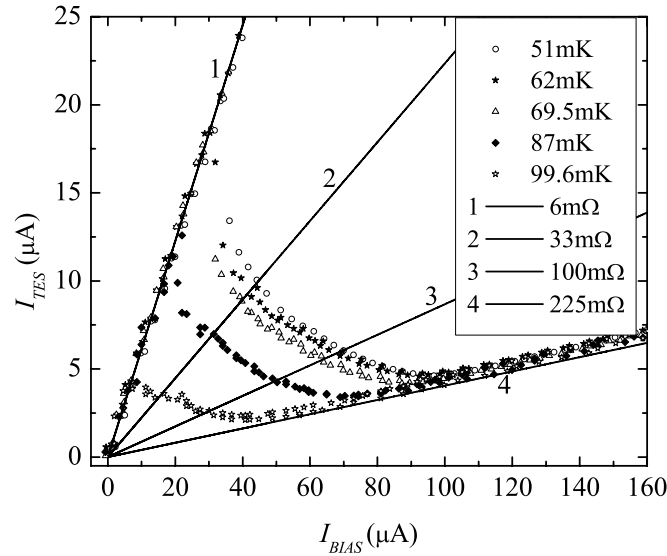


Fig. 3. – TES current *vs.* bias current at different temperatures (symbols as reported in the legend). Solid lines represent the current distribution for fixed resistance values (as reported in the legend) of TES branch.

3. – Results

The photon counting experiment, for the case of Ti/Au TES, has been obtained with a bath temperature of our dilution refrigerator $T_{\text{bath}} = 51 \text{ mK}$ and a bias current $I_{\text{bias}} = 42 \mu\text{A}$. The detector has been irradiated with a monochromator coupled to a $50 \mu\text{m}$ core multimodal optical fiber. The current pulses for different photon energies between 800 nm and 200 nm are shown in fig. 4. Fitting the pulse for an UV radiation

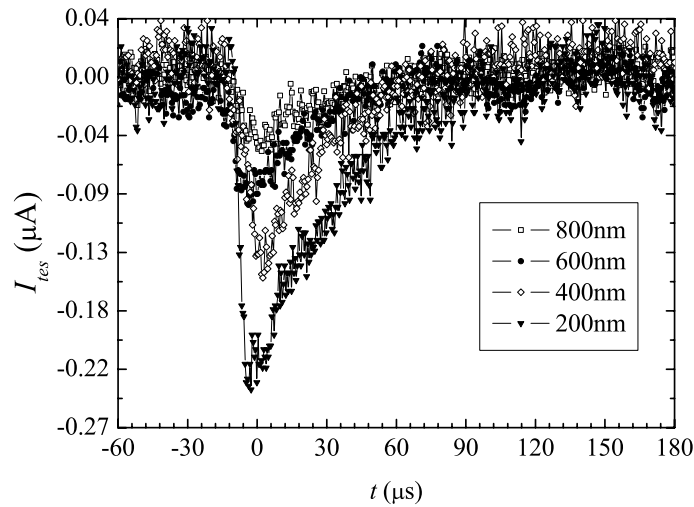


Fig. 4. – Current pulses, averaged over 10 samples, from 200 nm to 800 nm incident photons.

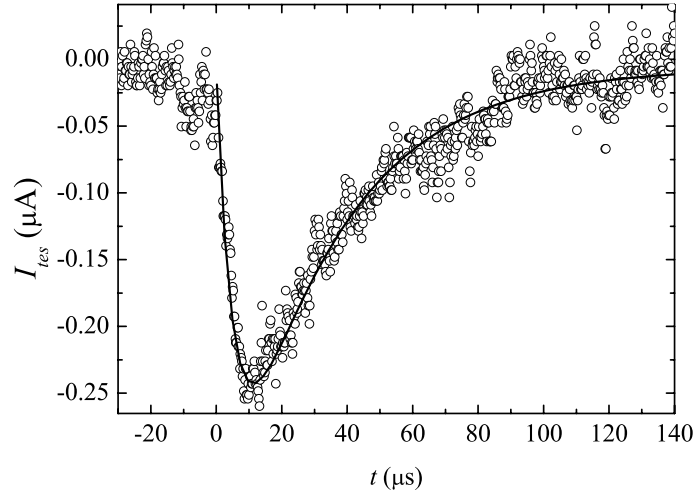


Fig. 5. – Current pulse for 200 nm photon event (dots) and its best fit (solid line) $A\left(e^{-\frac{(t-t_0)}{\tau_{\text{etf}}}} - e^{-\frac{(t-t_0)}{\tau_{\text{el}}}}\right) + B$ with an exponential rise $\tau_{\text{el}} = 32 \mu\text{s}$ and a decay time constant $\tau_{\text{etf}} = 52 \mu\text{s}$.

at $\lambda = 200 \text{ nm}$ (fig. 5) with two exponential functions $A\left(e^{-\frac{(t-t_0)}{\tau_{\text{etf}}}} - e^{-\frac{(t-t_0)}{\tau_{\text{el}}}}\right) + B$, where A , B and t_0 are constant, we can estimate the rise time $\tau_{\text{el}} = 5 \mu\text{s}$ and the decay time $\tau_{\text{etf}} = 32 \mu\text{s}$.

In the case of Ti/Pd TES, the detector was irradiated with pulses $0.5 \mu\text{s}$ wide from a 690 nm modulated diode laser, attenuated by proper neutral density filters. Non-averaged current pulses corresponding to the absorption up to 5 photons are shown in fig. 6, while

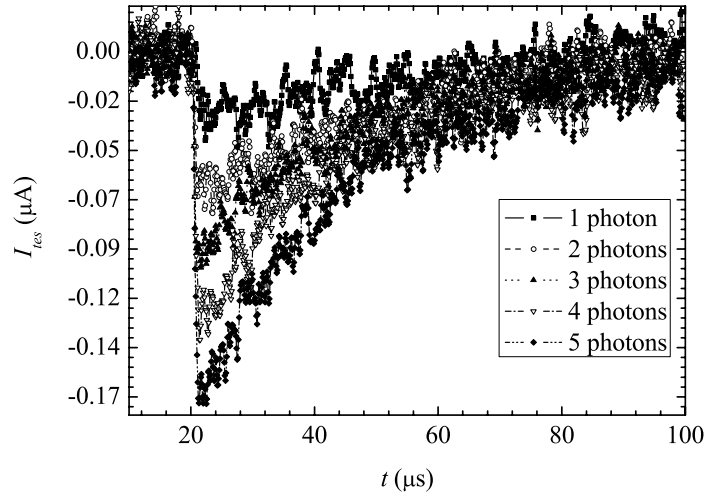


Fig. 6. – Current pulses, without any averaged over the samples, corresponding to 1-5 incident photons at 690 nm.

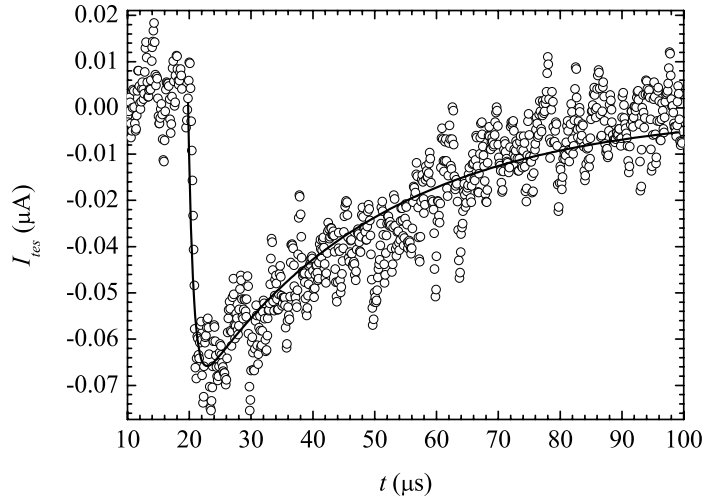


Fig. 7. – Current pulse for two-photon event (dots) and its best fit (solid line) $A \left(e^{-\frac{(t-t_0)}{\tau_{\text{eff}}}} - e^{-\frac{(t-t_0)}{\tau_{\text{el}}}} \right) + B$ with an exponential rise $\tau_{\text{el}} = 0.83 \mu\text{s}$ and a decay time constant $\tau_{\text{eff}} = 30 \mu\text{s}$.

in fig. 7, the current pulse related to two photons absorption is fitted with the aforementioned two-exponential function characterized by $\tau_{\text{eff}} = 21.7 \mu\text{s}$ and $\tau_{\text{el}} = 1.10 \mu\text{s}$.

While the effective response time of the two detectors are comparable, the Ti/Pd TES rise time is faster due to the higher value of the resistance at the working point.

4. – Conclusion

In this work we presented single-photon counting in the UV-visible range performed with superconducting Transition-Edge Sensors based on Ti bilayers, working at $\sim 100 \text{ mK}$. These detectors show an intrinsic energy resolution, and working at fixed wavelengths have a photon-number detection capability. This performance is particularly important for metrology and quantum technologies. The obtained results are strictly dependent on the detector heat capacity. To improve our results we are going to fabricate thinner and smaller sensors.

* * *

This work was supported by Piedmont Region project E45, call 2004.

REFERENCES

- [1] *Proceedings of the Single Photon Workshop 2007*, *J. Mod. Opt.*, **56**, nos. 1,2 (2009).
- [2] PORTESI C., TARALLI E., ROCCI R., RAJTERI M. and MONTICONE E., *J. Low Temp. Phys.*, **151** (2008) 261.
- [3] MONTICONE E., TARALLI E., PORTESI C. and RAJTERI M., to be published in *J. Phys. Conference Series*.
- [4] IRWIN K. D., *Appl. Phys. Lett.*, **66** (1995) 1998.

- [5] IRWIN K. D. and HILTON G. C., *Cryogenic Particle Detection*, edited by ENSS C. (Springer-Verlag, Berlin Heidelberg) 2005, pp. 63-149.
- [6] IRWIN K. D. and HILTON G. C., *Topics Appl. Phys.*, **99** (2005) 63; CABRERA B. and ROMANI R. W., *Topics Appl. Phys.*, **99** (2005) 417.
- [7] KNEIP G. D., BETTERTON J. O. and SCARBROUGH J. O., *Phys. Rev.*, **130** (1963) 1687.